

Scanning probe with an integrated diamond heater element for nanolithography

著者	小野 崇人
journal or publication title	Applied Physics Letters
volume	82
number	5
page range	814-816
year	2003
URL	http://hdl.handle.net/10097/35788

doi: 10.1063/1.1541949

Scanning probe with an integrated diamond heater element for nanolithography

Joon Hyung Bae^{a)} and Takahito Ono

Graduate School of Engineering, Tohoku University, 01 Aza Aoba, Aramaki, Aoba-ku, Sendai 980-8579, Japan

Masayoshi Esashi

New Industry Creation Hatchery Center, Tohoku University, 01 Aza Aoba Aramaki Aoba-ku, Sendai 980-8579, Japan

(Received 7 October 2002; accepted 9 December 2002)

This letter reports the microfabrication, evaluation, and application of a boron-doped diamond microprobe with an integrated resistive heater element. The diamond heater with a pyramidal tip, which is formed at the end of two diamond beams, can be electrically heated by a flowing current. The high thermal conductivity of the diamond base supporting the heater element allows very quick thermal response of 0.45 μ s. A hard-wearing sharp diamond tip formed by the silicon-lost mold technique shows excellent durability in contact operation with a sample. Diamond is well suited to use as a nanolithography tool for modification of a polymer, because polymer is hard to deposit on the tip during scanning due to the chemical inertness of the diamond surface. Demonstration of thermomechanical nanolithography with this heated probe exhibits line patterns with the feature size of 40 nm on a poly(methylmethacrylate) film. © 2003 American Institute of Physics. [DOI: 10.1063/1.1541949]

Scanning probe microscopy is increasing its demands not only as scientific tools but also as nano-engineering tools for nanolithography,¹⁻⁴ high-density data storage, manipulation,⁵ etc. As for the nanolithography, many articles have been published to show the ability of writing patterns in nanoscale. However, the durability of probes, reliability, and throughput in processing are still crucial problems in these applications. Despite scanning tunneling microscopy based lithography showing atomic scale resolution,⁶ the low processing speed limits its use because the time constant of the feedback circuit for keeping the tunneling current at a constant determines the maximum processing speed. Noncontact or tapping operations in scanning probe microscope and near-field scanning optical microscopy have same issue. Atomic Force Microscopy (AFM) operated in contact mode shows higher operating speed^{7,8} because it allows a wide dynamic range in operational force and does not need any electronics when it is operated without a feedback. The integrated AFM systems with actuators⁹ and probe array^{10,11} are developed toward actual utilization. In these systems, the simplicity of the operation of each probe is very important to intergrate an electric circuit into a microsystem for parallel operation. Thermomechanical writing method based on scanning thermal microscopy has been shown to be an effective method to modify a polymer film for high-density data storage.^{12,13} In this method, the thermoplastic polymer was locally heated by a heated tip above the glass melting points and thermomechanically deformed; the formed pits were defined by the feature size of the apex of the tip.

The contact-mode scanning methods have major disadvantages, i.e., break or abrasion of tips. Owing to its direct contact with a solid surface and iterative scanning, probe tips

were prone to be broken or worn out.¹⁴ It is widely known that diamond has good mechanical hardness and high thermal conductivity.¹⁵ Using diamond as a probe material, it is expected to solve these problems in the contact operation.

This letter describes the fabrication and the characterization of the scanning thermal probe made of boron-doped diamond. This diamond probe is demonstrated for use in thermomechanical nanolithography on a thermoplastic polymer film. As shown in Fig. 1, the resistive diamond heater element with a pyramidal tip was formed at the end of two beams. The length and the width of the beams are 300 and 40 μ m, respectively. The size of the heater element is 15 μ m \times 10 μ m \times 3 μ m. All of the beams, the heater elements, and the tip were made of boron-doped diamond. These beams were supported by the base of Pyrex glass in which feedthrough holes were formed for electric contact. By flowing current into two beams, the heater element including a tip can be heated up by Joule heat.

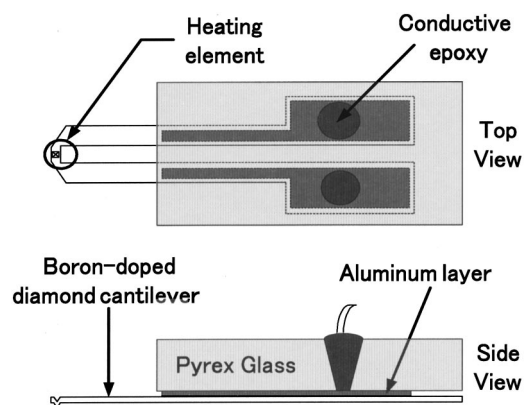


FIG. 1. The schematic structure of the boron-doped diamond probe.

^{a)}Electronic mail: icyce@mems.mech.tohoku.ac.jp

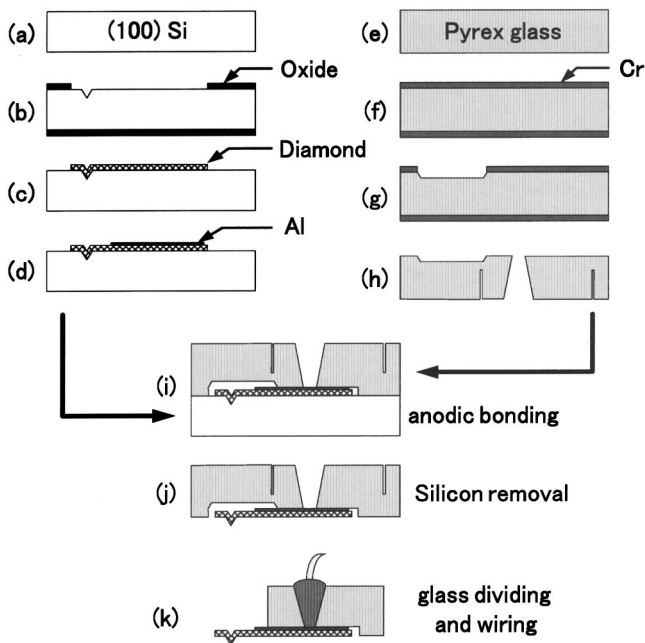


FIG. 2. Simplified process chart for a boron-doped diamond probe.

The combination of a silicon lost-mold technique and selective growth of diamond, as shown in the fabrication sequence in Fig. 2, was used for making sharp tips and diamond structures. A *p*-type (100)-oriented silicon wafer with 5–8 Ω cm was oxidized and the oxide was patterned by photolithography. Using this oxide layer as a masking material, the silicon was anisotropically etched in 20 wt% KOH etchant at 80 °C to make a tip mold. Then a 3-μm-thick boron-doped diamond was selectively deposited on the silicon using hot-filament chemical vapor deposition (HF-CVD),^{16,17} where a mixture of CH₄ (1.5%) and hydrogen is introduced at the total gas pressure of 5.2 KPa through mass flow controllers and activated by a heated tungsten filament at 2000 °C. An additional small amount of vaporized tri-methoxyborane as a boron source is introduced at the same time. To ensure the selective growth of diamond, deposition process was carried out as follows. First, the silicon substrate with a patterned oxide was treated for diamond nucleation using an ultrasonic agitator with 1 μm diameter of diamond powders. Then oxide layer was slightly etched in

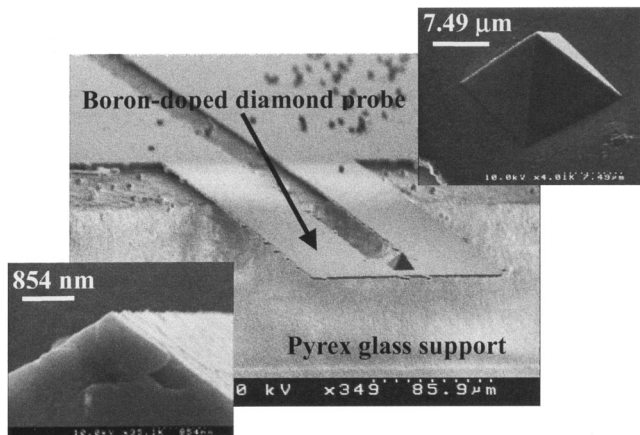


FIG. 3. SEM views of the fabricated boron-doped probe and the tip.

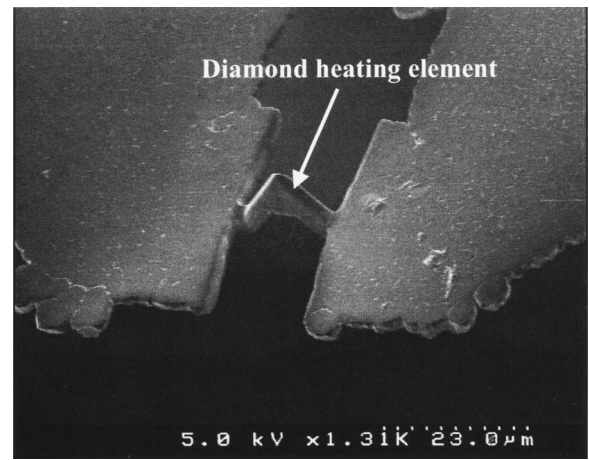


FIG. 4. The modified diamond heater by FIB milling.

buffered HF (BHF). This process selectively removed the diamond nucleation on the oxide layer. A 300-nm-thick Al pattern was formed on diamond by sputtering and following photolithography, which serve as an adhesive intermediate layer for anodic bonding with the Pyrex glass or as an optical mirror at the end of cantilevers for optical displacement sensing. Pyrex glass with a thickness of 0.3 mm was processed as shown at the right-hand side of Fig. 2. Part of the glass, which corresponds to the upper areas of the cantilever beams after bonding, was selectively etched in BHF with a masking Cr pattern. Feedthrough holes with a diameter of 400 μm and narrow Grooves with a depth of 150 μm were formed by a drilling machine and dicing saw, respectively. The silicon and Pyrex glass were bonded together using anodic bonding technique under a voltage of 600 V at 500 °C. Then, silicon mold was etched with inductively coupled plasma-reactive ion etching using SF₆ gas, and cantilevers were released. The probe array was cut into a piece along the glass grooves, and metal wires were glued onto the holes with a conductive adhesive. Scanning electron microscopy (SEM) observations were undertaken to evaluate the completed devices. Figure 3 shows the SEM images of the probe and the apex of the tip. Most of diamond probe tip has the tip apex of about 80 nm in diameter. In addition, focused ion beam (FIB) milling can exactly define and modify the heater structure. The front and back of the pyramidal tip on the diamond heating element

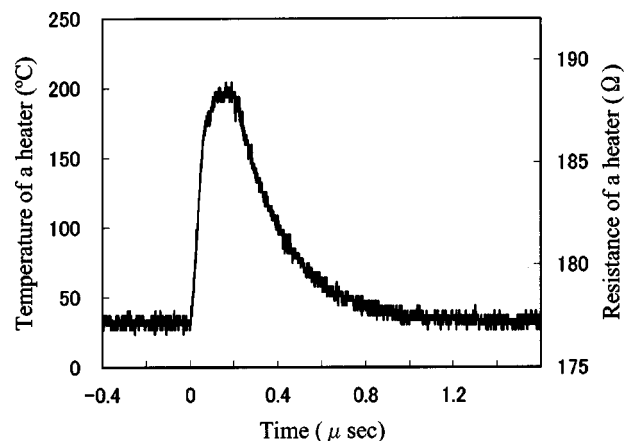


FIG. 5. Thermal response of the heater elements when a pulse voltage was applied. The temperature change estimated from the resistance was plotted.

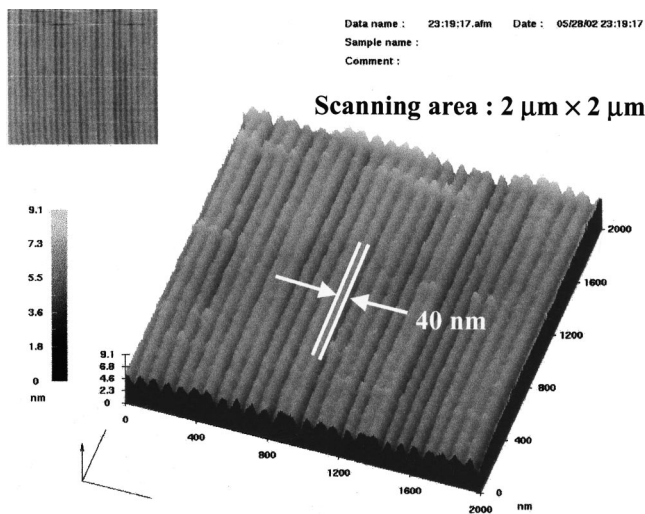


FIG. 6. Thermomechanically formed pattern on a thin PMMA film.

were removed for making a narrow heating element in $2\ \mu\text{m}$ width, as shown in Fig. 4.

Thermal properties of the diamond probe were characterized from the thermal response of the probe. From the measurement of I - V characteristics, the resistivity of CVD diamond is estimated to be $3.2 \times 10^{-3}\ \Omega\ \text{cm}$ at room temperature if the contact resistance was supposed to be ignored. The thermal response time of the heater was measured from the decay curve of the resistance when pulse voltage was applied.¹⁸ Figure 5 shows the decay curve of resistance and corresponding temperature. In Fig. 5, the temperature was estimated from the measurement result of the probe resistance versus temperature where a 4 V pulse with a pulse width of $0.2\ \mu\text{s}$ was applied. From this result, it can be seen that the diamond probe shows the thermal response time of about $0.45\ \mu\text{s}$. Here we defined the thermal response time as the falling time from 90% to 10% of the maximum resistance. Analysis with finite element method using Ansys® was conducted on the heater element with the same dimension, which shows the thermal response time of $0.5\ \mu\text{s}$ when the thermal conductivity of the CVD diamond was assumed to be $9\ \text{W/cm K}$.¹⁹ It should be noted that the thermal response of diamond structure is much higher than that of silicon with the same size (about $5\ \mu\text{s}$). The dissipated heat will conduct from the heater to the beams made of diamond. The large thermal conductivity of diamond enables us to shorten the thermal response time.

Thermomechanical nanolithography was demonstrated on a 100-nm-thick poly(methylmethacrylate) (PMMA) film. Diamond probe scanned on the PMMA coated silicon sample with applying a dc or ac voltage to the heater at a constant force on the order of $1\ \mu\text{N}$. Demonstrated diamond cantilever has a resonant frequency of 215 kHz and a spring constant of 20 N/m. First, with applying dc voltage of 4 V to the diamond cantilever (expected to be heated at 200°C), the diamond probe scanned on the sample and modified the sur-

face. Then, using the same probe, an AFM image of the modified surface was undertaken. As shown in Fig. 6, narrow lines with a width of 40 nm and a depth of 7 nm were formed.

Pits were formed on the PMMA by pulse heating of the heater as well, and the fabricated pit pattern was transferred onto a silicon substrate by dry etching. The array of pits was formed by applying pulse voltages to the diamond probe (amplitude: $5.2\ V_{p-p}$, frequency: 250 Hz) in scanning with the speed of $100\ \mu\text{m/s}$. Pit patterns with a diameter of 230 nm and a pitch of 400 nm were transferred onto a silicon substrate by etching with a fast atom beam using the PMMA as a mask. With the previously measured thermal response time of the diamond probe, the maximum scanning speed for making pit patterns with the pitch of 400 nm can be estimated to be about 0.8 m/s, which is two times faster than that reported in Ref. 20. Furthermore, the high processing speed can be realized with the parallel operation of diamond probe array, which is our research theme under development.

In summary, the boron-doped diamond probe with a sharp stylus was fabricated and applied to thermomechanical nanolithography. Abrasion was not recognized due to the superior mechanical properties of the diamond tip. Furthermore, a high-speed nanolithography process can be realized due to the large thermal conductivity of diamond probe.

- ¹P. Davison, A. Lindell, T. Makela, M. Paalanen, and J. Pekola, *Microelectron. Eng.* **45**, 1 (1999).
- ²R. Magno and B. R. Bennett, *Appl. Phys. Lett.* **70**, 1855 (1997).
- ³A. Golzhauser, *Appl. Surf. Sci.* **141**, 264 (1999).
- ⁴F. S.-S. Chien, C.-L. Wo, Y.-C. Chou, T. T. Chen, S. Gwo, and W.-F. Hsieh, *Appl. Phys. Lett.* **75**, 2429 (1997).
- ⁵M. Guthold, G. Matthews, A. Negishi, R. M. Taylor II, D. Erie, F. P. Brooks, and R. Superfine, *Surf. Interface Anal.* **27**, 437 (1999).
- ⁶J. A. Stroschio and D. M. Eigler, *Science* **254**, 1319 (1991).
- ⁷R. C. Barrett and C. F. Quate, *J. Vac. Sci. Technol. B* **9**, 302 (1990).
- ⁸S. Hosaka, A. Kikukawa, H. Koyanagi, T. Shintani, M. Miyamoto, K. Nakamura, and K. Etoh, *Nanotechnology* **8**, 58 (1997).
- ⁹H. J. Mamin, H. Birk, P. Wimmer, and D. Rugar, *J. Appl. Phys.* **75**, 161 (1994).
- ¹⁰M. I. Lutwyche, M. Despont, U. Drechsler, U. Durig, W. Haberle, H. Rothuizen, R. Stutz, R. Widmer, G. K. Binnig, and P. Vettiger, *Appl. Phys. Lett.* **77**, 3299 (2000).
- ¹¹D. W. Lee, T. Ono, T. Abe, and M. Esashi, *J. Microelectromech. Syst.* **11**, 215 (2002).
- ¹²H. J. Mamin and D. Rugar, *Appl. Phys. Lett.* **61**, 1003 (1992).
- ¹³M. Despont, J. Brugger, U. Drechsler, U. Durig, W. Haberle, M. Lutwyche, H. Rothuizen, R. Stutz, R. Widmer, G. Binnig, H. Rohrer, and P. Vettiger, *Sens. Actuators* **80**, 100 (2000).
- ¹⁴M. J. Madou, *Fundamentals of Microfabrication*, 2nd ed. (CRC, Boca Raton, FL, 2002).
- ¹⁵E. Kohn, P. Gluche, and M. Adamschik, *Diamond Relat. Mater.* **8**, 934 (1999).
- ¹⁶H. E. Hintermann, *Mater. Sci. Eng., A* **209**, 366 (1996).
- ¹⁷E. Oesterschulze, W. Scholz, Ch. Mihalcea, D. Albert, B. Sobisch, and W. Kulisch, *Appl. Phys. Lett.* **70**, 435 (1996).
- ¹⁸C. H. Mastragelo, J. H.-J. Yeh, and R. S. Muller, *IEEE Trans. Electron Devices* **ED-39**, 1363 (1992).
- ¹⁹K. M. Leung, A. C. Cheung, B. C. Liu, H. K. Woo, C. Sun, X. Q. Shi, and S. T. Lee, *Diamond Relat. Mater.* **8**, 1607 (1999).
- ²⁰B. W. Chui, T. D. Stowe, Y. S. Ju, K. E. Goodson, T. W. Kenny, H. J. Mamin, B. D. Terris, R. P. Ried, and D. Rugar, *J. Microelectromech. Syst.* **7**, 69 (1998).